

Simulation study on discrete charge effects of SiNW biosensors according to bound target position using a 3D TCAD simulator

This content has been downloaded from IOPscience. Please scroll down to see the full text.

2012 Nanotechnology 23 065202

(<http://iopscience.iop.org/0957-4484/23/6/065202>)

View [the table of contents for this issue](#), or go to the [journal homepage](#) for more

Download details:

IP Address: 140.113.28.197

This content was downloaded on 12/12/2014 at 08:31

Please note that [terms and conditions apply](#).

Simulation study on discrete charge effects of SiNW biosensors according to bound target position using a 3D TCAD simulator

In-Young Chung¹, Hyeri Jang², Jieun Lee², Hyunggeun Moon¹,
Sung Min Seo³ and Dae Hwan Kim²

¹ Department of Electronics and Communications, Kwangwoon University, Kwangwoon-ro 20, Nowon-gu, Seoul 139-701, Korea

² School of Electrical Engineering, Kookmin University, 861-1, Jeongneung-dong, Seongbuk-gu, Seoul 136-702, Korea

³ DRAM Design Team, Memory Division, Samsung Electronics, San 16 Banwol-Dong, Hwasung-City, Gyeonggi-Do 445-701, Korea

E-mail: drlife@kookmin.ac.kr

Received 22 September 2011, in final form 6 December 2011

Published 17 January 2012

Online at stacks.iop.org/Nano/23/065202

Abstract

We introduce a simulation method for the biosensor environment which treats the semiconductor and the electrolyte region together, using the well-established semiconductor 3D TCAD simulator tool. Using this simulation method, we conduct electrostatic simulations of SiNW biosensors with a more realistic target charge model where the target is described as a charged cube, randomly located across the nanowire surface, and analyze the Coulomb effect on the SiNW FET according to the position and distribution of the target charges. The simulation results show the considerable variation in the SiNW current according to the bound target positions, and also the dependence of conductance modulation on the polarity of target charges. This simulation method and the results can be utilized for analysis of the properties and behavior of the biosensor device, such as the sensing limit or the sensing resolution.

(Some figures may appear in colour only in the online journal)

1. Introduction

Silicon nanowire field effect transistors (SiNW FET) are among the leading candidates for a transducer in a label-free biosensor. The label-free electrical biosensor takes advantage of the field effect induced by charges of target biomolecules in an electrolyte environment. Receptor probes are immobilized on the surface of an SiNW so that the target molecules are bound to the probes by the bio-affinity phenomenon. The target charges induce the field effect on the SiNW channel that leads to the current conductance modulation. Numerous experimental works have shown the basic biosensing operation and have demonstrated the possibility of this type of biosensor [1–7]. While a considerable amount of

experimental results have been accumulated, analytic analyses remain insufficient such that some biosensor characteristics are not yet clearly interpreted. The domain of the biosensor system includes very different types of material regions, such as semiconductor, electrolyte solution and organic molecule regions. Moreover, the biosensors often have very complicated geometries. For this reason, an analytic study on the biosensor behavior has been regarded as a very challenging work. There have been some pioneering analytical studies on the SiNW FET as the transducer of a biosensor, giving fundamental understanding of the biosensor behavior [8, 9]. They have successfully modeled the field effect in a biosensor environment by taking the screening effect into account. However, the one-dimensional modeling

where a uniform density of the sheet charge covering the entire SiNW surface is assumed can scarcely be expanded to a higher dimension due to the inherent complexity. Therefore, they have a limitation in quantifying the sensing effects or interpreting diverse biosensor characteristics. In actuality, the SiNW biosensors usually have 3D structures, and the finite-sized target molecules are randomly bound to the receptors. The conductance modulation effect induced by irregular charge distribution can scarcely be estimated through analytical methods. The irregular distribution of the target charge is likely to have more apparent effects in the condition of a very low target concentration where only a small portion of the receptor probes is bound to the target molecules. Only a numerical simulation method enables the detailed analysis of the effect of the actual charge distribution. For this reason, simulation approaches have also been attempted [10, 11]. The most serious problem encountered during the assembly of the simulator is that the electrostatics of semiconductor and electrolyte regions are described by different equations. Variable boundary conditions are used on the electrolyte-to-semiconductor interface to cope with this problem. The potential (ϕ_s) or the electric field on the interface surface computed from the electrolyte solver is handed over to a semiconductor solver as the boundary condition. However, such a method, in practice, requires an assumption about the initial boundary condition on the interface, which is somewhat incorrect, when solving the electrostatics of the electrolyte region.

In this paper, we construct a biosensor simulation method using a well-established commercial semiconductor simulator, known as the TCAD tool, which can deal with 3D structures. This simulation method deals with a simulation domain that includes both semiconductor and electrolyte regions. The electrolyte solution is considered as a type of semiconductor material in which the hole and electron charges represent the mobile ions in the solution. Though most electrical properties of the electrolyte may not agree with those of the modeled semiconductor material, such as the charge mass and mobility, the electrostatic distribution of the mobile charges can be accurately computed with the semiconductor model, which determines the field effect of the SiNW biosensor. The electrolyte region can be presumed to be electrically static in a DC simulation condition where all electrodes are DC biased. The modulation of the SiNW DC current due to charges in the electrolyte region is directly simulated without interface parameters. Therefore, various biosensor characteristics can be reproduced using this simulation method, such as the sensitivity and the current fluctuation as well as various environmental effects, including the screening effect. After introducing the simulation method, we report various types of electrostatic simulation results, thus giving valuable insight into the biosensor mechanism.

2. Simulation method

We use a commercial 3D TCAD tool (Sentaurus, Synopsys Inc.) for the biosensor simulation [12]. While the electrical properties of semiconductors and dielectric materials have

been accurately modeled, the TCAD simulator cannot yet deal with the ionic solution. However, the DC conductance of the SiNW biosensor, i.e. the field effect induced by the target charge, can be reproduced if the relevant charge distribution in the ionic solution region is provided. We define the ionic solution as an intrinsic semiconductor material with the dielectric constant of water in this simulation method. In a real ionic solution, the charge distribution in the electric double layer is represented by the Poisson–Boltzmann (PB) equation [13]. If we assume a 1:1 electrolyte (e.g. $K^+ - Cl^-$), the original form of the PB equation can be written as below:

$$\frac{\partial^2 \phi}{\partial x^2} = -\frac{q}{\epsilon} \left\{ C_0^{K^+} \exp\left(-\frac{q\phi}{kT}\right) - C_0^{Cl^-} \exp\left(\frac{q\phi}{kT}\right) \right\} \quad (1)$$

where $C_0^{K^+}$ and $C_0^{Cl^-}$ denote the K^+ and Cl^- ion concentrations at the electrically neutral condition, having the same value between them. This PB equation is very close to the semiconductor equation except for the Fermi–Dirac distribution of the hole and electron charges in the semiconductor. The semiconductor equation applied in an intrinsic material can be rearranged as follows:

$$\frac{\partial^2 \phi}{\partial x^2} = -\frac{q}{\epsilon} \left\{ p_0 \frac{1 + e^{\frac{E_i - E_v}{kT}}}{1 + e^{\frac{E_i - E_v}{kT}} e^{\frac{q\phi}{kT}}} - n_0 \frac{1 + e^{\frac{E_c - E_i}{kT}}}{1 + e^{\frac{E_c - E_i}{kT}} e^{-\frac{q\phi}{kT}}} \right\}. \quad (2)$$

In this equation, p_0 and n_0 respectively denote the hole and electron concentrations in the neutral condition. Equation (2) accords very well with equation (1) if $(E_g/2 - q\phi)$ is greater than a few thermal energies (kT), an assumption which is always satisfied in our simulation conditions. If we replace the electrolyte solution with an intrinsic semiconductor, the electrostatic solution of the electrolyte region can be calculated by solving the semiconductor equation at the region.

Since we model the ionic solution as an intrinsic semiconductor, we must decide a few more physical parameters for the semiconductor material. First, we specify the bandgap of the semiconductor as the silicon bandgap (1.12 eV) because the bandgap has only to satisfy the condition $(E_g/2 - q\phi) \gg kT$. Second, the equivalent density of state (DOS) of the semiconductor (N_c , N_v) is determined such that the number of the hole and electron charge is equal to the molal concentration of solution ions. Third, the electron affinity (χ_e) also should be determined such that the simulation reproduces the real I – V characteristics of the SiNW device. The electrochemical meaning of electron affinity is related to the standard reduction potential between the silicon and the ionic solution. In the aspect of the electrostatic simulation, however, the electron affinity is referred to determining the flat-band voltage of the gating material. Thus, the change in the χ_e of the solution material leads to the same magnitude of the V_{LG} shift in the I_D – V_{LG} (drain current–liquid gate voltage) characteristics as shown in figure 1(a). We have determined the χ_e value from the experimental results. Our research group fabricated SiNWs similar to the device to be simulated in this work. We performed the I_D – V_{LG} simulations of the SiNW device with the ionic solution gate by altering the χ_e value as shown

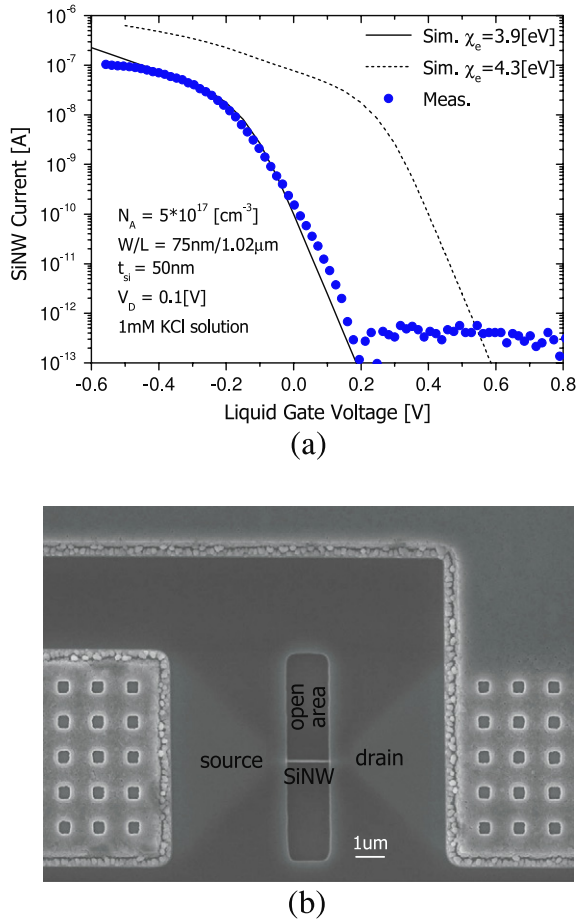


Figure 1. (a) Simulated SiNW I_D – V_{LG} characteristics with $\chi_e = 3.9, 4.3$ (eV) in comparison with the measured results. Simulation details are described afterwards. (b) The SEM image of the fabricated SiNW device used for the I – V measurement in (a).

in figure 1(a). We found that the simulated I_D – V_{LG} curve shows the best fit to the measured curve when χ_e is 3.9 eV. It is obvious that the measured SiNW device contains an amount of charges in the oxide and the interface region. However, these are all put together effectively into the χ_e value of the simulation. Because the χ_e only shifts the I_D – V_{LG} characteristics, the estimated χ_e value, though not so rigorous from the perspective of physics, would not be much of a problem for the simulation studies in this work.

Semiconductor charges are different from the mobile ions in that their sizes are infinitely small. The spatial distribution of the ion charges in dilute solution can be reduced to the following equation by the Debye–Hückel theorem [14]:

$$\ln \gamma = -\frac{z^2 q^2}{8\pi \epsilon (\lambda_D + r_0) kT} \quad (3)$$

where γ , λ_D , ϵ , r_0 , zq and kT denote the ion activity, the Debye length, permittivity, the radius of the ion, the ion charge and the thermal energy, respectively. The ion activity, γ , is the property proportional to the ion concentration in a dilute solution. It is found in equation (3) that the effect of the finite ion size can be neglected if the Debye length is much greater than the ion size. Actually, the Debye length in dilute solution

(1 mM) at 300 K is 9.6 nm while the ion size is around 0.5 nm [15, 16]. Since the Debye length increases as the ion concentration decreases, the finite ion size can be neglected unless the ion concentration is very high.

Let us discuss the limit of the validity of the simulation method using these parameters. The upper bound of the range of ion concentrations may be around 500 mM where the Debye length becomes comparable to the ion size. The lower bound is associated with the dimension of the simulation domain because the simulation domain of the solution region can be smaller in size than the Debye length, and also with the bandgap of the solution material because the potential applied to the double-layer capacitance of the solution region can exceed half of the bandgap. It should be noted that the parameters for the simulation of the solution material, such as χ_e , are not derived from physical properties. Instead, they can be considered as a kind of fitting parameter to reproduce the electrostatics in the solution region and the SiNW DC current in TCAD simulations, which many factors contributing to the I – V characteristics such as the interface charges are equivalently put together in. In addition, the shape of the simulated SiNW device, being different from the actual SiNWs which usually have round edges and rough surfaces, can also be a cause of simulation error.

3. Target charge models

As viewed from a system standpoint, the concentration of target molecules and the conductance modulation of SiNW correspond respectively to the input and the output of the biosensor system. Conductance modulation should be an indicator of the concentration of target molecules. Experimental works have demonstrated that a higher concentration of target molecules generally leads to a greater degree of current modulation [4, 17–19]. Thus, the SiNW conductance simulation depending on the target charge density would be the basic simulation for the analysis of biosensor characteristics, which we term as the ‘static transfer’ simulation.

For the static transfer simulation of the SiNW biosensor, a relevant charge model to represent the actuality of the bound target charges should be provided. In many studies, the target charge density is simplified to be spatially uniform over the entire FET transducer device and regarded as a continuous variable depending on various factors such as the target concentration in the solution. A more realistic model of the target charges can be described as a cluster of charges on the surface of a target molecule which is bound randomly to a receptor site. When a binding reaction occurs at a certain position on the SiNW surface, a finite-sized charge cluster becomes attached to the position. In actual cases, the target charge density can have only two states, target-bound or target-less, at a specific point. Instead of a spatially uniform and continuous increase in the target charge density, the area of the target-bound surface increases as more binding events occur. Thereby the target charge is distributed over the SiNW surface irregularly with granularity of the molecular size.

In contrast to the FET device where the surface potential of the entire channel region is consistently controlled by the gate voltage, the biosensor transducer does not have such a consistent surface potential profile over the entire channel region. The local channel conduction is modulated by nearby charges, and the overall SiNW conductance is decided by synthesizing all such modulation effects. The effects caused by this non-uniformity in the surface charge condition can be estimated numerically with the relevant charge model.

In order to construct the relevant charge model, we start with the simple uniform sheet charge (USC) model. In the USC model, the target charge layer is defined as a 2 nm thick dielectric sheet covering the whole top surface of the SiNW channel region. The charges are uniformly distributed across the whole sheet region and the charge density is treated as a continuous variable. This model is similar to the charge condition assumed in the 1D analysis. We also introduce the uniform discrete charge (UDC) model to take into account the effect of the clustered charge, where the receptor site is described as a dielectric cubic volume. As the binding events occur to the receptors, the dielectric cubes are supposed to become charged. In this UDC model, however, all dielectric cubes on the SiNW surface are assumed to have the same charge density. Another model reflecting the irregular distribution of the bound targets is the random discrete charge (RDC) model. There exist two states of the dielectric cubes, corresponding to the receptor sites, in this model. A finite amount of charges ($\pm Q_T = \pm 1.2 \times 10^{-16}$ C in our work) is assigned only to the cubic volume which has captured the target molecule. Since the binding event may occur to a part of the receptor sites, an SiNW biosensor has both charged and uncharged cubes simultaneously. The schematic illustration of the three charge models is shown in figure 2.

It may not be an accurate description that the receptor is cubic-shaped and that charges are uniformly spread across the entire receptor–target molecule for the discrete charge models. However, we assume here that the shape of the charged volume does not critically affect the biosensor characteristics. The receptor molecule often has its own charges, causing a shift to the DC I – V characteristics of the SiNW FET, similar to the fixed oxide charges of the FET device. Nonetheless, it remains unchanged that the change in the charge amount of the receptor–target molecule due to the binding reaction induces conductance modulation to the SiNW by the field effect.

4. Simulations

The SiNW FET, used in the biosensor simulations, is based on the SOI (silicon-on-insulator) structure in which 100 nm of buried oxide (BOX) is between the SiNW channel and the back substrate region. The SiNW has a 5×10^{17} -doped p-type channel between the highly doped p+ source and drain regions. The width, height and length of the SiNW channel are 75 nm, 50 nm and $1.025 \mu\text{m}$, respectively. The channel region of $0.925 \mu\text{m}$ is exposed to the solution with unexposed 50 nm channel extensions on both sides, connected to the source and

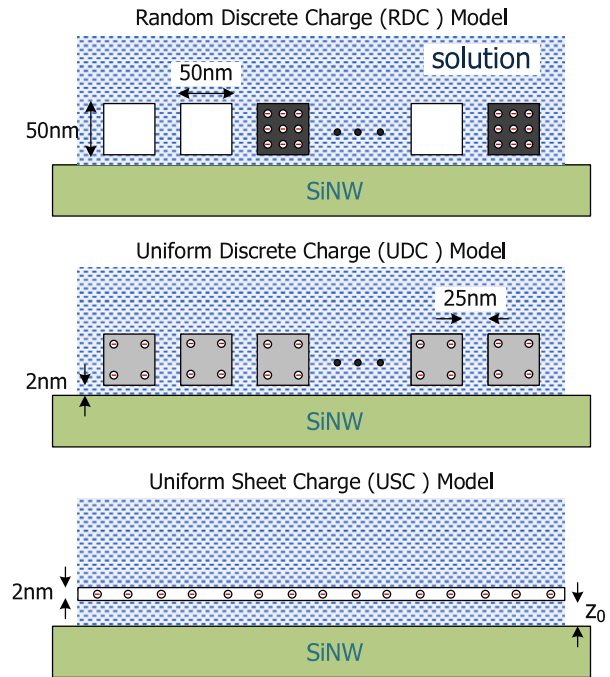


Figure 2. Schematic diagrams of the three target charge models used in this simulation work.

drain regions. The exposed channel region has 3 nm thick surface oxide.

The simulation domain comprises the SiNW (source, drain and channel regions), the buried oxide and back-gate regions, an adequate volume of the solution regions. The top surface of the solution volume is defined as the electrode of the solution material. Since the vertical thickness of the simulated solution region is 250 nm, much greater than the Debye lengths in these simulations, this constant-potential boundary condition is consistent with the actual state in the bulk solution region. As the Neumann boundary condition is applied to the side facets of the simulated solution volume, fringing effects may be excluded in these simulations. To obtain the SiNW conductance in the linear mode, the DC simulation is performed with a small drain bias (<100 mV). The solution and the back gate are biased to fixed voltages so that the SiNW channel is partially depleted where higher sensitivity is achieved [10].

There are several types of biosensor probes from a small molecule to an antibody according to the target material, whose physical sizes range from several to tens of nanometers [4]. Considering the mesh size related to the efficiency of the simulations, we assume a large size of the receptor–target molecules. The receptor cubes used in the RDC and UDC models are defined as $(50 \text{ nm})^3$ cubics 2 nm apart from the oxide–electrolyte interface and surrounded by the solution material, representing that the bound targets are a few nanometers away from the sensor surface by a linker or receptor molecule [20]. We assume 12 evenly spaced receptor cubes only on the top surface of the exposed SiNW channel region for convenience of simulation, with 25 nm gaps between the two neighboring receptors. The receptors cover about 43% of the top surface area, which

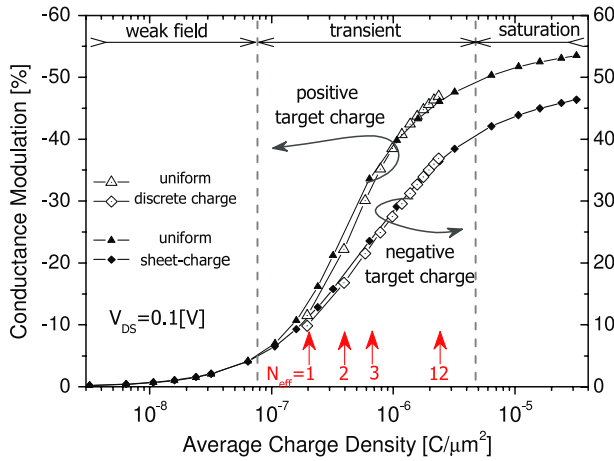


Figure 3. SiNW conductance simulations depending on the target charge density, i.e. static transfer simulation results with the UDC model and with the USC model. N_{eff} points indicate the average charge density that N_{eff} of 12 receptor sites capture targets charged with $\pm 1.2 \times 10^{-16}$ C.

is an acceptable value according to the random sequential adsorption (RSA) model [21, 22]. In the RDC model, the receptor cube has no net charge before it captures the target molecule and becomes charged to $-Q_T = -1.2 \times 10^{-16}$ C (or $Q_T = +1.2 \times 10^{-16}$ C) when the receptor captures the target molecule. The charge value, Q_T , is assigned so that the charged receptor cube gives the charge density per unit surface area of the SiNW, comparable to that given by the streptavidin molecule in pH7 solution. It is a very simplified description about the geometry of the target charge, compared to the complicated real charged molecules. However, considering the trade-off between the simulation performance and the accurate description of the charged molecule, this simplification is inevitable for simulation efficiency and also acceptable for the analysis of the tendency of biosensor characteristics depending on various parameters.

First, we performed the static transfer simulations with the USC and UDC models. Figure 3 shows the ratios of conduction modulation as a function of the target charge densities averaged over the whole top surface. The x -axis values of 12 points, simulated with the UDC model, correspond to the average charge densities of $\pm Q_T/WL$, $\pm 2Q_T/WL$, ..., $\pm 12Q_T/WL$, where WL means the top surface area of the exposed SiNW channel region. The conductance modulation ratios of the USC model fit best to those of the UDC model at the same average charge densities when the geometrical parameter, z_0 in figure 2 is 10 nm, meaning that the equivalent distance of the cubic target charges is around 10 nm from the SiNW surface. The simulation results in figure 3 show the typical S-shaped curves commonly found at measurement of the electrical biosensors [18].

Figure 4 shows several features of the electrostatic simulation with the RDC model. Figure 4(a) presents an overview of the simulation domain with three captured target molecules, where the thin oxide regions are not visualized. Figure 4(b) presents a cross-sectional view with charge density contours in the silicon and solution regions.

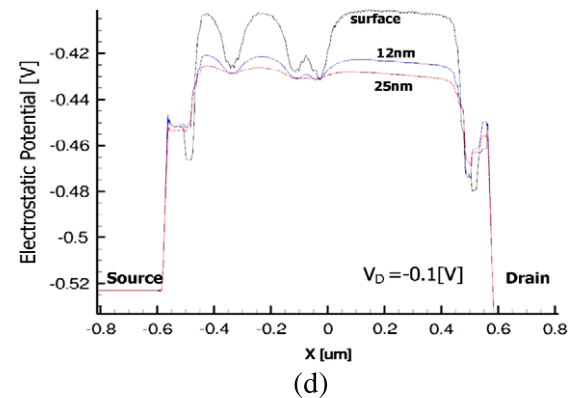
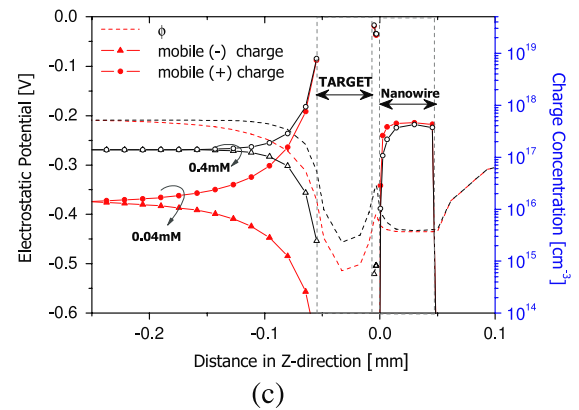
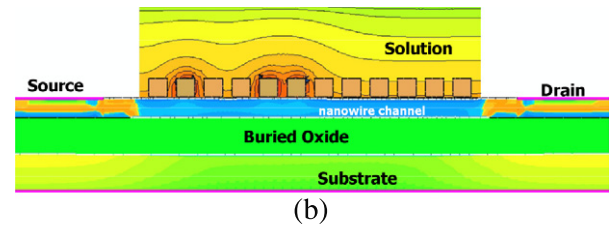
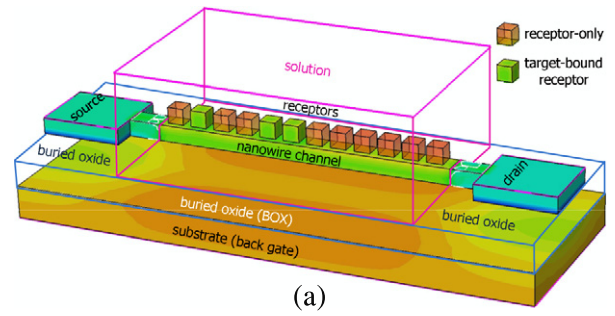
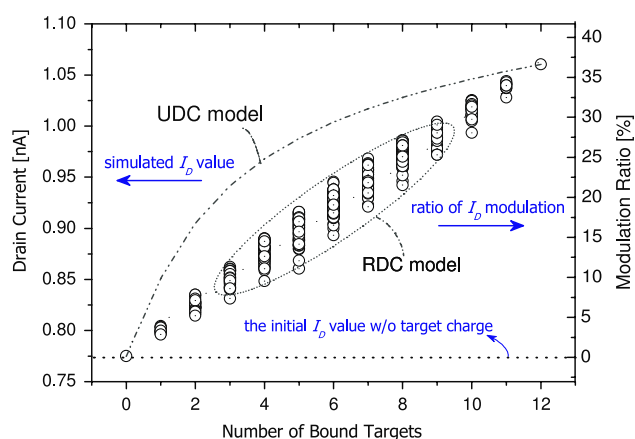


Figure 4. (a) An overview of the biosensor used in this simulation work, assuming that 3 of 12 receptors capture the target molecules, (b) a cross-sectional view of the biosensor device in (a) with the mobile positive charge concentration contours, (c) the potential and mobile charge concentration profiles along the z direction at the solution ion concentrations of 0.04 and 0.4 mM conditions, and (d) the channel potential plots from the source to the drain according to the distance from the SiNW top surface.

Figure 4(c) shows the potential and the mobile charge concentration profiles along the z direction, clearly visualizing the double layers in the solution region depending on the ion concentration, which causes the field screening effect.

Table 1. Numbers of simulation sample cases according to the captured target number.

Number of bound targets	0, 12	1, 11	2, 10	3, 9	4, 8	5, 7	6
Number of binding cases	1	12	66	220	495	792	924
Number of simulation samples	1	12	27	39	50	75	87
Proportion (%)	100	100	40	18	10	9.5	9.4

**Figure 5.** SiNW current modulations depending on the number of bound target charge (static transfer characteristics), simulated with the RDC model in comparison with the UDC model. Each target is charged with -1.2×10^{-16} C.

This figure shows that charge concentrations converge to their neutral values with decay constants of the Debye lengths calculated as 19 nm and 56 nm at ion concentrations of 0.4 mM and 0.04 mM, respectively. We observe very high ion concentrations in the 2 nm gap space between the receptor cubes and the SiNW surface, as ascribed to the deeper negative potential in the gap region due to incomplete field screening in the $+z$ direction. The electrostatic potential along the channel is plotted in figure 4(d) depending on the distance from the top surface. The potential acts as a barrier height for the p-type FET, through which the current conductance is exponentially reduced. When approaching from the surface to the center point of the SiNW cross section, the potential becomes lower and less modulated. It is well known that a thinner transducer device having a higher ‘surface-to-volume ratio’ is more sensitively modulated by surface reactions, which is implied in this profile plot as well.

The static transfer characteristics of the SiNW are simulated with the RDC model when the captured target number increases from 1 to 12. In the RDC model, however, the static transfer cannot be represented by a single curve. The SiNW can have a different conductance value depending on the bound target positions despite the fact that it has the same number of bound targets. Because the conductance does not have a linear relationship to the target charge, overall conductance modulation cannot be obtained through a linear summation of the modulation effects induced by each target. Therefore, we must simulate every case of the receptor–target binding combination to obtain a complete set of conductance results, which, however, is not an efficient method. Instead, we

simulated several randomly selected sample cases to obtain the static transfer. It is well known in statistics that the mean and variance of a sample group can represent those of all cases if the number of samples is sufficiently large. We increase the number of simulation sample cases as the number of all binding cases increases, as shown in table 1.

Figure 5 shows the static transfer plot with the RDC model, simulated with a charge of $-Q_T$ per target molecule and with a 0.04 mM solution ion concentration. Even a single target modulates the conductance by about 4%. While simulations with the UDC model result in a logarithmic-like transfer curve, the mean conductance has a linear relationship with the target number in this RDC model. Of course, this does not indicate a linear relationship between the conductance modulation and the target concentration in the electrolyte. The number of bound targets in a steady state is a function of several factors as well as the target concentration in the solution [23]. The RDC model identifies one source of biosensor noise and assists with the analysis of the current fluctuation in the SiNW sensors. As shown in figure 5, conductance variations in cases with the same target number may be greater than the conductance difference between two cases having different target numbers. The current variation given the same target number is regarded as an additional noise source, which introduces a fundamental limit to the accuracy of the biosensor system, where the solution target concentration and the conductance modulation are the system input and output, respectively. There are a couple of rules about the effect of charge on the current modulation. Generally, charge on the source side has a greater influence on the SiNW conductance than the charge on the drain side. The second cubic charge from the source end most modulated the conductance while the last one (12th in this simulation) least modulated the current. The distribution of the charge cubes also has a large influence on the current modulation. The SiNW current is more modulated when the charges are evenly distributed than when they localize at a certain part.

The current sensitivity, $\Delta I/I$, depends on the bias condition. Figure 6 plots the ratios of the current modulations according to the target number, simulated with -25 and -100 mV drain voltages, showing that a lower drain voltage is advantageous in terms of sensitivity. The target on the drain side has a weaker effect as the drain voltage becomes higher. However, the low drain voltage reduces the current magnitude so as to degrade the signal’s noise immunity against environmental noise.

Figure 7 shows that the FET biosensor sensitivity depends on the charge polarity, especially when the number of bound targets is small. In the case of positive target charges, the static transfer of the RDC model is relatively close to that

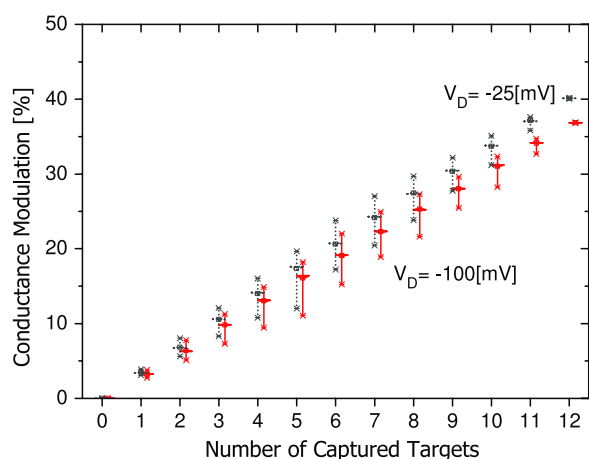


Figure 6. The static transfers depending on the drain biases. The mean points and the min–max ranges are denoted in this plot.

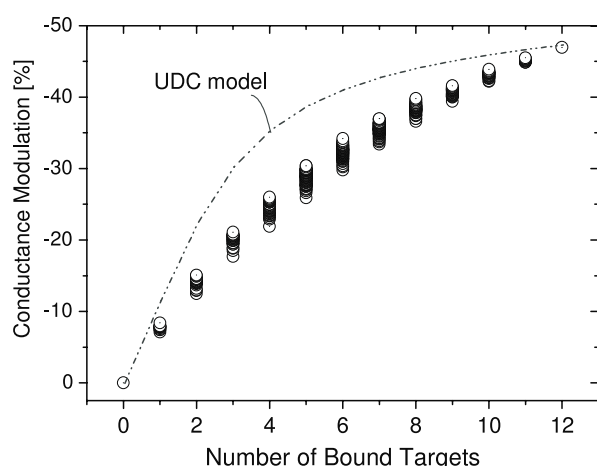


Figure 7. The static transfer simulations with the RDC model when each target is charged with $+1.2 \times 10^{-16}$ C.

of the UDC model. For the p-type SiNW, the conductance is more sensitive to positive charges than the same amount of negative charges when the number of captured targets is small. In addition, the variation is suppressed. This can be explained in terms of the series connection effect of the local transistors. Supposing that the SiNW channel is sliced by a small unit length, it can be regarded as a series connection of the unit ‘local-FETs’. While this does not have a significant influence on the entire conductance to lower the resistance of one ‘local-FET’, the increased resistance of one ‘local-FET’ can dominate the entire resistance value. These results provide insight into the design of SiNW biosensors in which the sensor devices should have majority carriers of the same polarity as the target charge in order to obtain good sensitivity.

We also investigated the effect of the solution ion concentration on the biosensor sensitivity. We simulated the static transfer characteristics depending on the ionic concentration in the solution. Figure 8 shows that the conductance modulation decreases more rapidly as the ionic concentration becomes higher, implying that the ionic concentration is the critical condition for high sensitivity. However, the variations are reduced even more at higher concentrations, such that the conductance ranges overlap

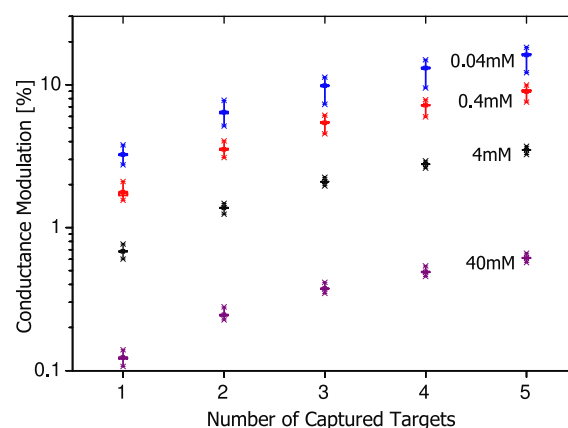


Figure 8. The conductance modulations depending on the solution ion concentrations.

slightly between the different target numbers. The range that the electric field reaches is reduced to a very small area such that there is little interaction between the target fields.

In our simulation works, we assumed that the target charges are uniformly distributed over the entire receptor–target cube in the discrete charge models, which may not agree with the actual condition. If the target is bound onto the top of the receptor molecule, most target charges are likely to be located at the upper part of the molecular cube. Thus, the actual screening effect may be stronger than the simulated effect.

5. Conclusion

We introduced a biosensor simulation method dealing with the semiconductor and the electrolyte region together using the well-established semiconductor 3D TCAD simulator tool. Through the simulation method, we conducted biosensor DC simulations with a charge model where the receptor–target molecule is described as a dielectric cubic volume with a charge density, located randomly across the SiNW surface. The simulation results showed that the drain current fluctuates depending on the positions of the bound targets and that the transfer characteristics depend on the charge polarity. The simulation method and results can be utilized for analyses of the properties and behaviors of SiNW biosensors, such as the sensing limit and the sensing resolution. The influences of device parameters and environmental conditions on the biosensor sensitivity can also be predicted with this simulation method. We expect that this simulation work will contribute to the development of a design guide for sensitive and reliable biosensor devices.

Acknowledgments

This work was supported by the Basic Science Research Program (no. 2010-0023999) and by the Mid-career Researcher Program (no. 2010-0027649) through an NRF grant funded by the MEST. The present research was also conducted by the Research Grant of Kwangwoon University in 2010.

References

- [1] Cui Y, Wei Q, Park H and Lieber C M 2001 *Science* **293** 1289–92
- [2] Stern E, Klemic J F, Routenberg D A, Wyrembak P N, Turner-Evans D B, Hamilton A D, LaVan D A, Fahmy T M and Reed M A 2007 *Nature* **445** 519–23
- [3] Ahn J, Choi S, Han J, Park T J, Lee S Y and Choi Y 2010 *Nano Lett.* **10** 2934–8
- [4] Curreli M, Zhang R, Ishikawa F N, Chang H, Cote R J, Zhou C and Thompson M E 2007 *IEEE Trans. Nanotechnol.* **7** 651–67
- [5] Zheng G, Patolsky F, Cui Y, Wang W U and Lieber C M 2005 *Nature Nanotechnol.* **23** 1294–301
- [6] Kim A, Ah C S, Yu H Y, Yang J, Baek I, Ahn C, Park C W, Jun M S and Lee S J 2007 *Appl. Phys. Lett.* **91** 103901
- [7] Li Z, Chen Y, Li X, Kamins T I, Nauka K and Williams R S 2004 *Nano Lett.* **4** 245–7
- [8] Nair P R and Alam M A 2008 *Nano Lett.* **8** 1281–5
- [9] Nair P R and Alam M A 2010 *Appl. Phys. Lett.* **107** 064701
- [10] Nair P R and Alam M A 2007 *IEEE Trans. Electron Devices* **54** 3400–7
- [11] Wang Y and Li G 2010 *Proc. 10th IEEE Int. Conf. on Nanotechnol.* pp 1036–9
- [12] *Sentaurus User's Manual* v. D-2010-03 Synopsys Inc.
- [13] Grahame D C 1947 *Chem. Rev.* **41** 441–501
- [14] Atkins P and Paula J D 2006 *Physical Chemistry* (Oxford: Oxford University Press)
- [15] Marcus Y 1983 *J. Solution Chem.* **10** 271–5
- [16] Batsanov S S 1963 *J. Struct. Chem.* **4** 158–60
- [17] Kim A, Ah C S, Park C W, Yang J, Kim T, Ahn C, Park S H and Sung G Y 2010 *Biosens. Bioelect.* **25** 1767–73
- [18] Soleymanil L, Fang Z, Sargent E H and Kelley S O 2009 *Nature Nanotechnol.* **4** 844–8
- [19] Bunimovich Y L, Shin Y S, Yeo W S, Amori M, Kwong G and Heath J R 2006 *J. Am. Chem. Soc.* **128** 16323–31
- [20] Stern E 2007 Label-free sensing with semiconducting nanowires *PhD Thesis* Yale University
- [21] Evans J W 1993 *Rev. Mod. Phys.* **65** 1281–329
- [22] Lee K, Nair P R, Scott A, Alam M A and Janes D B 2009 *J. Appl. Phys.* **105** 102046
- [23] Squires T M, Messinger R J and Manalis S R 2008 *Nature Biotechnol.* **26** 417–26